

RESEARCH ARTICLE

Impacts of the Madden-Julian Oscillation on the intensity and spatial extent of heavy precipitation events in northern Northeast Brazil

Francisco das Chagas Vasconcelos Junior¹  | Charles Jones² |
Adilson W. Gandu³ | Eduardo Sávio P. R. Martins¹

¹Ceará Institute for Meteorology and Water Resources (FUNCEME), Fortaleza, Brazil

²Department of Geography and Earth Research Institute, University of California, Santa Barbara, California

³Departamento de Ciências Atmosféricas, Instituto de Astronomia, Geofísica e Ciências Atmosféricas, Universidade de São Paulo, São Paulo, Brazil

Correspondence

Francisco das Chagas Vasconcelos Junior, Ceará Institute for Meteorology and Water Resources, Funceme, Rui Barbosa, 1246 Fortaleza CE, Brazil.

Email: francisco.vasconcelos@funceme.br

Funding information

NOAA, Grant/Award Number: NA10OAR4310170; FAPESP, Grant/Award Numbers: 2013/09642-5, 2011/09314-2

Abstract

This paper investigates the spatiotemporal variability of Contiguous Extreme Precipitation Events (CEPE) related to Madden-Julian Oscillation (MJO) activity during the pre-wet season and wet season in northern Northeast Brazil for 30 years (1979–2010). Inherent differences in rainy season regimes are associated with northern Northeast Brazil precipitation systems; these are isolated during pre-wet and wet season and analyse the intensity and the spatial area covered by the CEPE. A daily index of MJO activity and its life cycle were used to identify activity phases during heavy rainfall events. Composite analysis was performed for days with CEPE during the most frequent MJO phases in the pre-wet and wet seasons. The analysis shows the influence of the MJO on the occurrence of CEPE in northern Northeast Brazil. In the pre-wet season, the MJO phases 8-1-2 affect the occurrence of heavy rainfall events, modifying the atmospheric circulation and water vapour transport over northern South America. Indications of Rossby wave propagation over the South Pacific associated with MJO were found, suggesting tropic-extratropic teleconnection during occurrences of CEPE in the pre-wet season. In the wet season, CEPE events are more frequent during MJO phases 8-2-3. Conversely, no wave propagation over the South Pacific is observed in the wet season, changes in wind anomalies at high and low atmospheric levels only point to the influence of the MJO via tropical teleconnection. This study may help monitoring and forecasting of very heavy rainfall events in northern Northeast Brazil in pre-wet season and wet season.

KEYWORDS

extreme rainfall, MJO life cycle, Northeast Brazil

1 | INTRODUCTION

Northeast Brazil is considered the poorest and third most populous region in Brazil and recurrent droughts have high socioeconomics impacts. Many observational and

modelling studies have investigated the influence of drought frequency-intensity, forecasting skill and anomalous atmospheric circulation patterns in the northernmost Northeast Brazil (NNB) (Namias, 1972; Hastenrath and Heller 1977, Moura and Shukla, 1981;

Hastenrath, 2006; Sun *et al.*, 2006; Rao *et al.*, 2006; Hastenrath, 2012). This area covers the most part of the region known as the “drought polygon” (Ramos, 1975) (Figure 1). While many papers have focused on the influence of interannual variations or intraseasonal modulation on rainfall variability, there is a lack of detailed investigations regarding the influence of intraseasonal variability on intensity and spatial extension of the rainfall extremes events in NNB. Northeast Brazil has a semi-arid climate with large spatiotemporal variability of precipitation. On average, the rainfall annual cycle over the northernmost portion has a well-defined Wet Season (WES) from February to May. The Intertropical Convergence Zone (ITCZ) is the main contributor to this climatic feature (Hastenrath and Lamb, 1978). In addition, a short rainfall period, called the Pre-Wet Season (PWS), occurs from November to January (Brito and Nobre, 1991; Vasconcelos Junior *et al.*, 2018). Upper level cyclonic vortices and cold front incursions are the main atmospheric systems controlling the variability of the WES (Kousky, 1979; Kousky and Alonso Gan, 1981). Spatially, annual precipitation of 2000 mm is observed in coastal regions and less than 500 mm in the interior region (Sertão).

On interannual timescales, the El Niño Southern Oscillation (ENSO) is the main mode of variability with strong ocean–atmosphere coupled influences on large-scale atmospheric circulation and regional scale precipitation patterns (Philander, 1983; Aceituno, 1988). Specifically, over the NNB, warm ENSO phases are

associated with small increases in intensity and decrease of the frequency of events about NNB, while during the cold phase it is observed increased frequency of extreme precipitation events (EPE) (Grimm and Tedeschi, 2009). However, ENSO has markedly modulated NNB precipitation fluctuation, occurring on an interannual and seasonal scale, and not as a direct generator mechanism of EPE (Liebman *et al.* Liebmann *et al.*, 2011), which occur on intraseasonal timescale.

This study focuses on spatiotemporal variability of contiguous regions of extreme precipitation events (CEPE), that is, concentrated intense rainfall events in space (see Jones and Carvalho, 2012 for details). On intraseasonal time scales, the Madden-Julian Oscillation (MJO) is the most prominent large-scale mode (Madden and Julian, 1972, 1994; Zhang, 2013). The MJO influences precipitation variability in North America (Jones, 2000; Jones *et al.*, 2004; Jones and Carvalho, 2012, 2014), South America (Carvalho *et al.*, 2004; Liebmann *et al.*, 2011), Central America (Cavazos and Rivas, 2004; Martin and Schumacher, 2011), Australia (Hendon and Liebmann, 1990), Asia (Zhang *et al.*, 2009; Xavier *et al.*, 2014) and Africa (Matthews, 2000; Mutai and Ward, 2000). Specifically, the MJO modulates convective activity and extreme daily rainfall activity in the South American Monsoon System (SAMS), South Atlantic Convergence Zone (SACZ) (Carvalho *et al.*, 2002; Jones *et al.*, 2004; Liebmann and Allured, 2005; Muza *et al.*, 2009), and EPE over the Northeast of Brazil (Carvalho *et al.*, 2004) during the austral summer. Although some studies have shown that the MJO life cycle modulates precipitation over the NNB (Valadão *et al.*, 2015; Shimizu and Ambrizzi, 2016; Valadão *et al.*, 2017), there have not been specific studies that investigated potential influences of the MJO on CEPE over the Northeast Brazil. Some studies suggest that intraseasonal variations can control precipitation during the PWS and WES (Souza and Ambrizzi 2006; Vasconcelos Junior *et al.*, 2018). Liebmann *et al.* (2011) suggested that MJO provides conditions for convective activity generating high daily accumulated precipitation values, although more detailed studies, especially linked to the spatial coverage of extremes events, are needed.

This paper is motivated by the limited understanding of the mechanisms by which the MJO controls EPE over the NNB. The specific questions investigated are: (a) does the MJO influence the intensity and area of EPE during PWS and WES? What is the influence of the MJO life cycle phases on CEPE during PWS and WES? What are the large-scale atmospheric patterns associated with the MJO and CEPE over the NNB during PWS and WES? This manuscript is organized as follows. Section 2 describes the data sets used, the methodology for

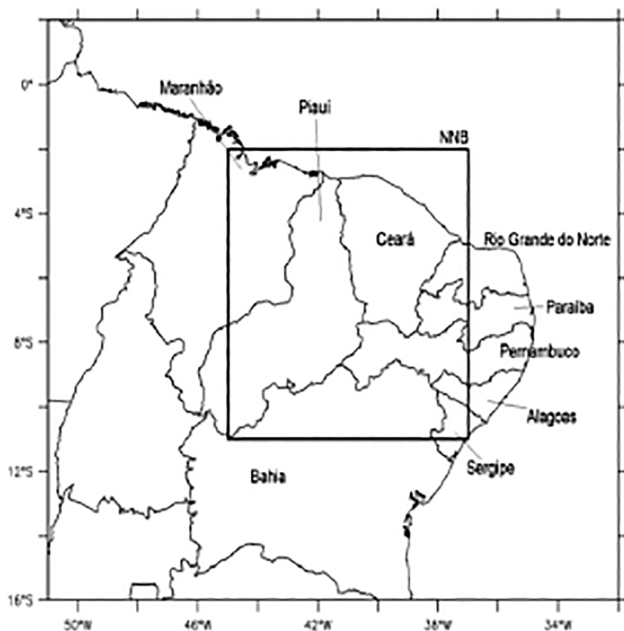


FIGURE 1 Northeast region of Brazil. The black square shows the study area of northern Northeast Brazil (NNB)

calculating CEPE and composite analysis. The main results and discussions are presented in Section 3. Summary and conclusions are presented in Section 4.

2 | DATA AND METHODS

2.1 | Data

This study focuses on the northern portion of northeast Brazil (NNB), which covers most of the semiarid region (Figure 1). Daily gridded rainfall over South America (1° latitude, longitude) is made available by NOAA and described in Liebmann and Allured (2005). It was used to investigate the spatiotemporal variability of EPE over the NNB. The analysis was performed for the period 1-Nov May 31, 1979–2010, this period was considered because it presents a greater amount of valid data and density of stations. Based on the study of Vasconcelos Jr et al. (Vasconcelos Junior *et al.*, 2018), the period from November to January refers to PWS, whereas the period from February to May refers to WES.

In addition, ERA-Interim Reanalysis (Dee *et al.*, 2011) during 1979–2010 (0.75° latitude, longitude) was used to characterize large-scale atmospheric circulation patterns. Daily averages of zonal and meridional wind components at 200-hPa and 850-hPa (U200, V200, U850, and V850), zonal and meridional components of the vertically integrated water vapour transport (Qx and Qy), and geopotential height at 200-hPa (H200) were used. Outgoing longwave radiation (OLR), this data was provided by NOAA (National Oceanic and Atmospheric Administration) and covers from 1979 to 2010, with grid spacing of 2.5 × 2.5° (Liebmann and Smith, 1996).

2.2 | Analysis procedure

2.2.1 | Identification of CEPE

To identify intensity and areas of EPE, Gamma frequency distributions were initially fitted to daily precipitation in each gridpoint in the analysis domain; only precipitation values above 0.1 mm were considered. The 75th and 90th percentiles of the intensity distribution were used to identify extreme precipitation. CEPE are defined as regions with spatially connected grid points in the daily precipitation exceeds the percentile thresholds of intensity. Connected points are those points that are in the vicinity forming a contiguous region of precipitation above the threshold for each point. This approach follows the methodology discussed in Jones and Carvalho (2012).

After identification of CEPE events, a frequency distribution of the size of the EPE was constructed (i.e., number of grid points in the contiguous area). The minimum and maximum sizes range from 1 grid point to the maximum number of gridpoints in the study area (Figure 1). To focus on extreme CEPE, two thresholds of 5 and 14 connected gridpoints were chosen; these thresholds correspond to the 75th and 90th percentiles of frequency distribution of connected grid points, respectively.

The geographic location of each CEPE occurrence was determined by the coordinates of the center calculated as the weighted average of total precipitation within the CEPE (Jones and Carvalho, 2012):

$$I_c = \frac{\sum_{i=1}^n iP_{ij}}{\sum_j P_{ij}} \quad J_c = \frac{\sum_{j=1}^n jP_{ij}}{\sum_j P_{ij}} \quad (1)$$

where n is the number of grid points in the CEPE, I_c and J_c are the longitude and latitude of the center and P_{ij} is precipitation in the grid point (i,j).

2.2.2 | Identification of MJO events and composite analysis

The identification of MJO events was performed with the daily index discussed in Jones and Carvalho (2012). The MJO index was computed using daily OLR, U850 and U200 data during January 1, 1979, to December 31, 2010. First, the annual cycle was removed from the time series and a band-pass filter was applied to retain intraseasonal variations in the 20–200 days scale. According to Matthews (2000), this procedure is more suitable to differentiate primary and successive MJO events. Next, the filtered OLR, U200 and U850 fields were equatorially averaged (15 N–15 S) and combined Empirical Orthogonal Functions (Wilks, 2011) were applied. The first two eigenvectors represent the eastward MJO propagation. The main differences from Wheeler and Hendon (2004) were the filtering procedure and identification of MJO events. Additional details can be found in Jones and Carvalho (2012).

Convective anomalies during the life cycle of the MJO are defined in eight phases according to filtered OLR composites during active MJO events (same analysis was performed by Jones and Carvalho, 2012) (Figure 2). It is important to note that when MJO convective anomalies are located over the Indo-Pacific region, suppressed convection is observed over northern South America (Phases 4 and 5). On the other hand, enhanced convection over South America and Tropical Atlantic is observed in Phases 1 and 8. Phases 2, 3, 6, and 7 are transition phases

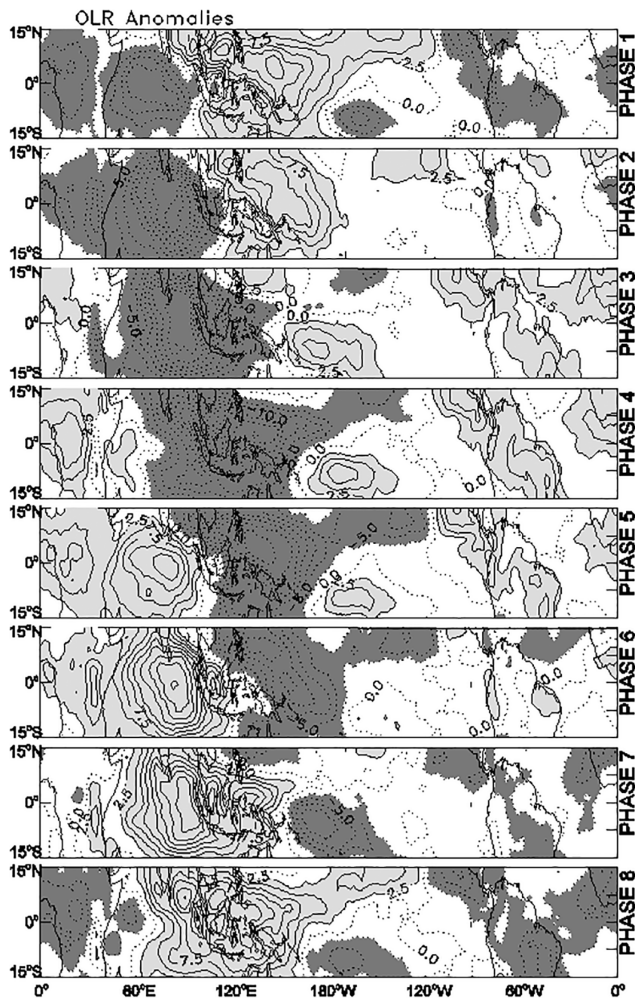


FIGURE 2 Composites of filtered OLR anomalies during MJO life cycle. Light (dark) grey depicts positive (negative) anomalies. Contour interval is 2.5 W/m²

between suppression and enhanced convection over northern South America.

CEPE was classified according to their occurrences during the year. Events occurring during November–January were assigned to PWS, whereas events happening during February–May were assigned to WES. Composites of unfiltered anomalies were also presented to demonstrate the influence of the MJO on the spatial variability of extreme precipitation. Only areas with statistical significance at 5% level based on Student’s *t* test are considered. The degrees of freedom for each point was calculated by $n-1$, where n is number of days with CEPE within the period covered by the chosen MJO phases.

3 | RESULTS AND DISCUSSION

Figure 3 shows the number of counts of CEPE events. Counts are assigned to centers of the CEPE. The total

number of CEPE exceeding 75th and 90th percentiles of spatial extent (number of connect grid points) were 3,789 and 477, respectively. Note that two or more CEPE can coexist within the study region on the same day. The maximum occurrences of CEPE in each percentile vary across the domain. The 75th percentile CEPE shows values above 100 over the State of Maranhão in the coastal region (Figure 3a), while the 90th percentile CEPE maximizes over southern Ceará State near the Araripe Plateau (Figure 3b). This suggests that mesoscale circulations and topographic effects have a strong control on the precipitation variability over the NNB. Here, we are particularly interested in investigating the role of the MJO in modulating CEPE occurrences.

The total number of CEPE was 2,281 during active MJO phases and 1,508 events during inactive MJO days for 75th percentile. For 90th threshold, we found 320 CEPE during MJO activity, while 157 events during inactive MJO. Figure 4a shows the proportions of CEPE during active and inactive MJO days for the 75th and 90th percentiles thresholds. The difference in proportions of CEPE during “MJO” and “no MJO” days are statistically significant at 5% level. These results confirm that the MJO plays an important role in enhancing atmospheric conditions favourable for the occurrences of CEPE in the NNB. The frequency distributions of CEPE according to MJO phases (Figure 4b) show that Phases 1, 2, and 3 have the highest occurrences of extreme events. In addition, MJO Phases 4, 5, and 6 show minimum occurrences. This result is consistent with the life cycle of the MJO because the effect of suppressing convective movements on the intraseasonal time scale on the northern sector of South America is found in the Phases 4, 5, and 6 (Figure 2). Phase 3 of MJO is a transition phase from favouring convection period to suppression of convection period. The index of the MJO was computed for daily time scale, where each phase lasts more than 5 days (on average is 6), the index should show Phase 1 or 2 in fact, but due to objective criteria to define each phase, it does not. The extreme events persist on time that do not necessarily start and end with the same phase of MJO. MJO drives the low circulation on vicinity of Northeast Brazil; it takes time for the extreme rainfall to occur. The correspondence between CEPE proportions and MJO phases is clearer for 90th percentile extremes, that is, very high extreme events are suitably associated with a differential role of the effects of MJO phases in contributing to convection in the study region during two distinct rainy seasons (PWS and WES) as discussed below.

Vasconcelos Jr et al. (Vasconcelos Junior *et al.*, 2018) showed that the precipitation variability over the NNB varies considerably during the PWS (NDJ) and WES

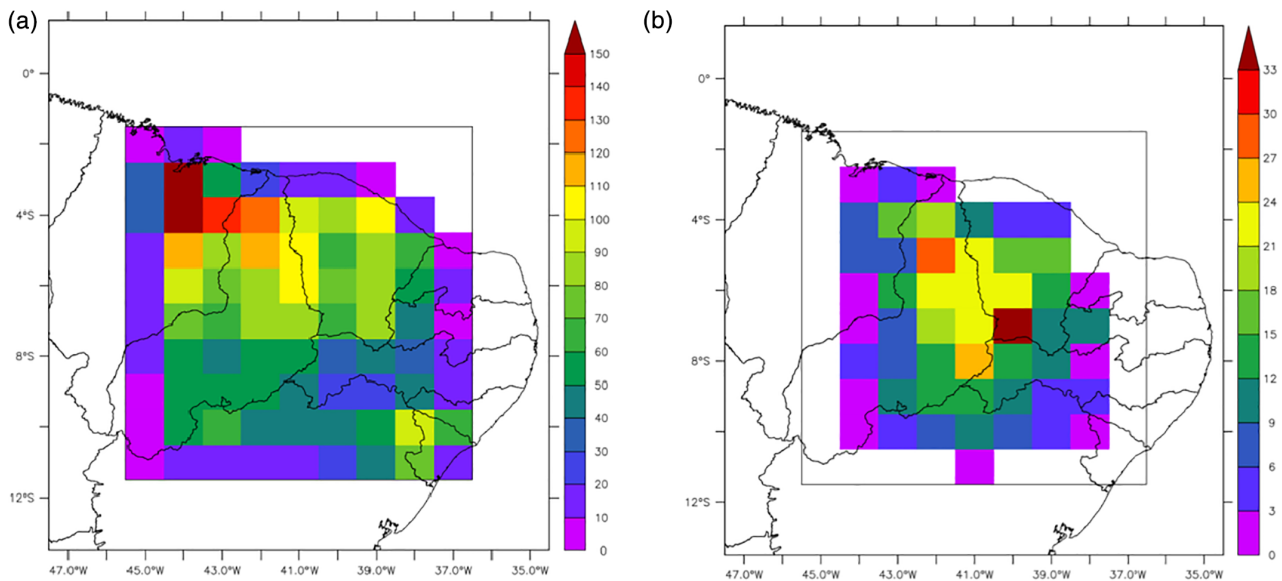


FIGURE 3 Counts of CEPE exceeding (a) 75th and (b) 90th percentile of intensity and area. Counts were assigned to the center of each CEPE during November 1, 1979 to May 31, 2010 [Colour figure can be viewed at wileyonlinelibrary.com]

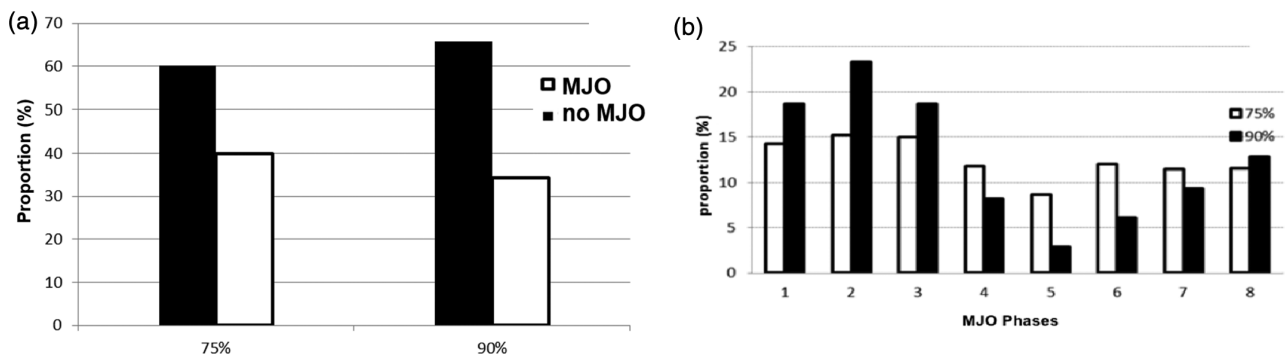


FIGURE 4 (a) proportion of CEPE for 75th and 90th percentile during days with active MJO (black bar) and no MJO (black bar) activity. (b) Proportion of CEPE for 75th and 90th percentiles during each phase of the MJO

(FMAM) periods. Figure 5 shows monthly proportions of CEPE occurrences for the two types of thresholds. Two maxima are observed in January and March. The first maximum is associated with the end of the PWS, while the second occurs within the WES. The maximum in March is associated with the southernmost position of the ITCZ (Hastenrath and Lamb, 1978).

To gain a better understanding on how extreme precipitation varies when the MJO is active, Figure 6 shows the proportions of CEPE occurrences for 75th and 90th percentiles during each MJO phase and separated by PWS and WES regimes. In the PWS regime, it is noticeable that the MJO has a larger modulation on 90th percentile CEPE than the 75th percentile CEPE (Figure 6a). Therefore, the large proportions occur in Phases 1 and 8, which is consistent with the MJO life cycle (Figure 2).

In the WES regime, the maximum occurs in Phase 3, which is also consistent because WES occurs after PWS.

To characterize the influence of the MJO on the occurrence of CEPE during PWS and WES, composites were divided into two periods: NDJ and FMAM. In the PWS regime, composites of 90th percentile CEPE events were calculated for MJO Phases 8-1-2, whereas for WES, composites were calculated for Phases 8-2-3. The results during the PWS are presented first followed by the WES analysis.

The divergence of vertically integrated moisture transport anomalies (Figure 7) shows large moisture convergence over eastern Brazil during 90th percentile CEPE occurrences in the PWS. Small areas of positive moisture transport divergence are observed over Indonesia, which are consistent with the MJO suppressed convection over

the maritime continent during Phases 8-1-2. Westerly wind anomalies at 850-hPa (Figure 8) are observed over the north-central parts of South America, which are part of a cyclonic circulation located over central Brazil. Figures 9 and 10 show composites of anomalies in wind at 200-hPa and geopotential height at 200-hPa, respectively.

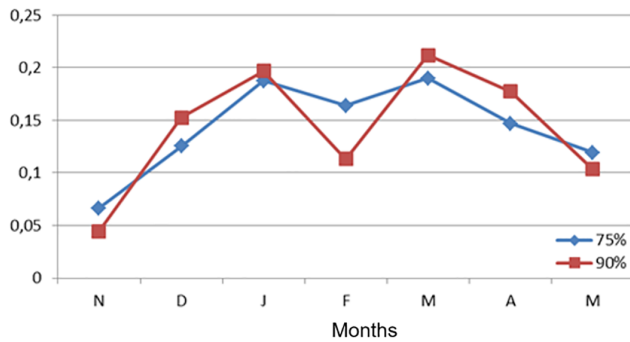


FIGURE 5 Proportion of days with CEPE occurrences during months from November to May above threshold of 75th and 90th [Colour figure can be viewed at wileyonlinelibrary.com]

The low-level cyclonic and anti-cyclonic circulation anomalies over South America are part of a Rossby wavetrain that originates from Indonesia. This large-scale remote forcing has been discussed in previous studies (Ambrizzi and Hoskins, 1997) including its control on precipitation variability over the SACZ (Liebmann *et al.*, 1999; Grimm and Tedeschi, 2009; Grimm, 2019). The novel aspect shown in this study is the linkage between the MJO and regions of extreme precipitation during the PWS over the NNB. The low-level cyclonic wind anomaly over eastern is consistent with Carvalho *et al.* (2004), who showed the existence of intraseasonal signals on episodes of intense precipitation over the SACZ.

To gain a better perspective on the temporal evolution of the MJO influence, Figure 11 shows lag composites of wind anomalies at 850-hPa. At lag -10 days, low-level cyclonic anomalies start to develop over southeastern Brazil and intensify at lag -5 days. As the enhanced convection associated with the MJO propagates eastward, the wavetrain is fully established at lag 0 days. At this

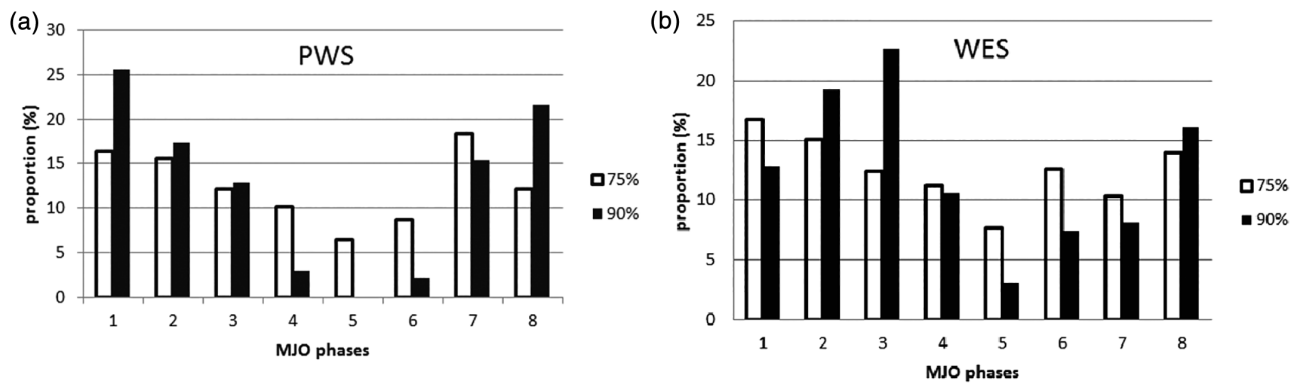


FIGURE 6 Proportion of CEPE for 75th and 90th during (a) the PWS and (b) the WES assigned to each MJO phase

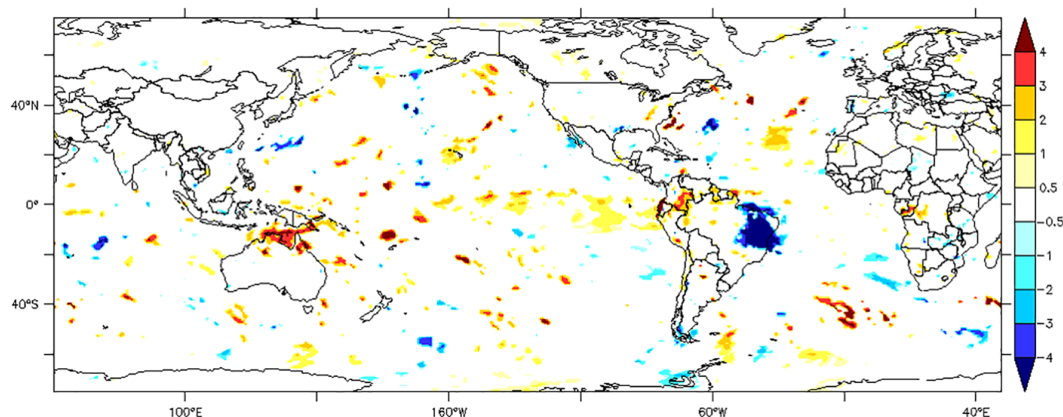


FIGURE 7 Composite of DIVQ anomalies (mm/day) during CEPE for 90th percentile within 8-1-2 MJO phases in the PWS. Just points with statistical significance at 5% level are shown [Colour figure can be viewed at wileyonlinelibrary.com]

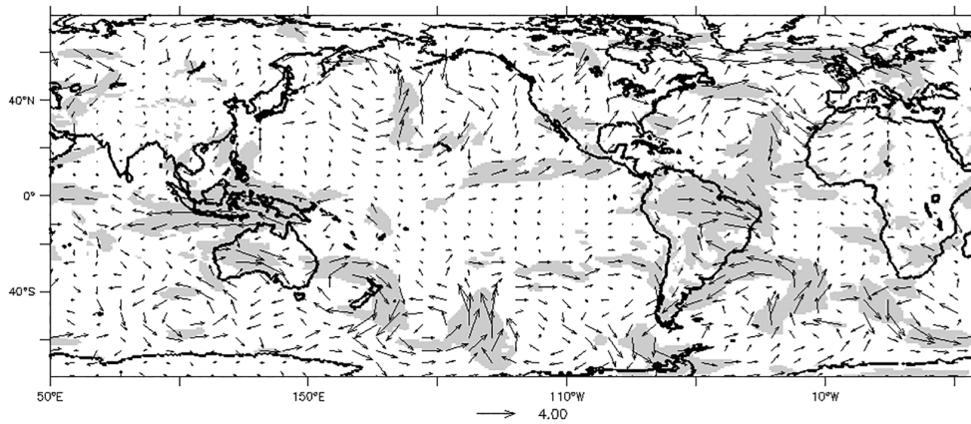


FIGURE 8 Composites of wind anomalies at 850 hPa during 90th CEPE percentile during MJO Phases 8-1-2 MJO during PWS. Regions with statistical significance at 5% level are grey colour

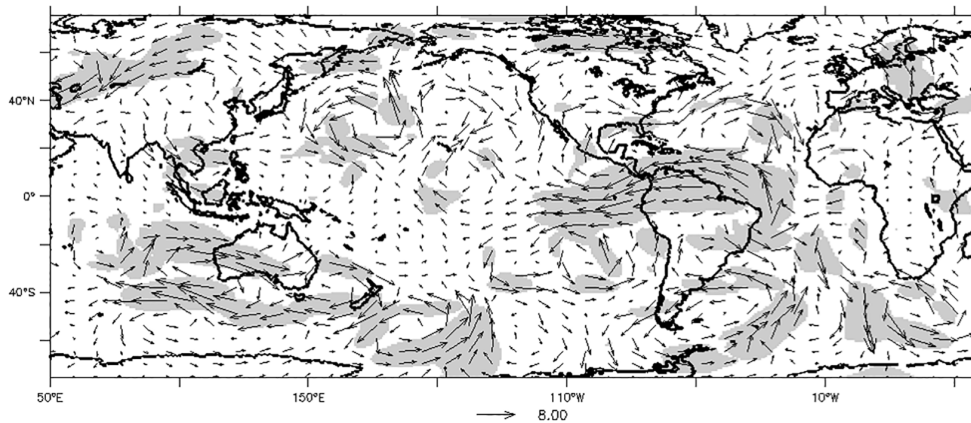


FIGURE 9 As Figure 8 except for wind at 200 hPa

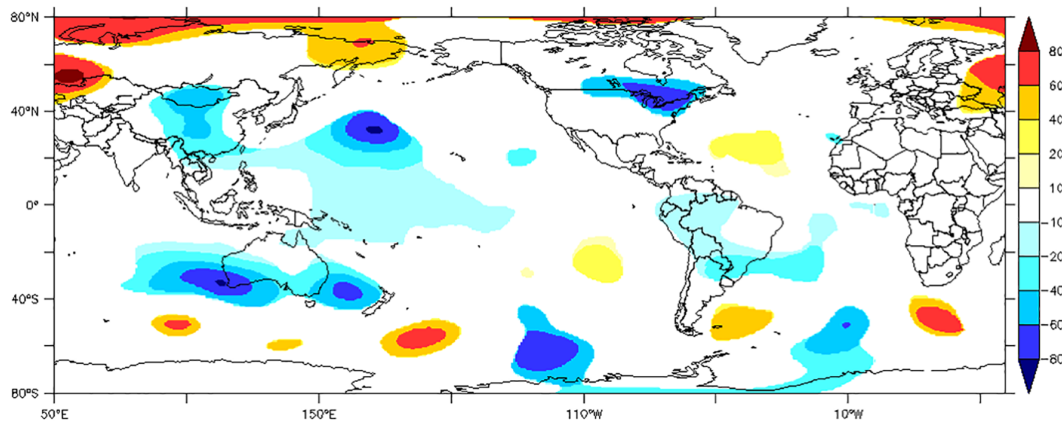


FIGURE 10 As Figure 8 except for H200 (m) [Colour figure can be viewed at wileyonlinelibrary.com]

time, the MJO has the maximum influence on CEPE over the NNB. At lag 5 days, the low-level cyclonic anomaly weakens as the favourable convection signal propagates eastward. This characteristic has already been indicated as suppression of SAMS and SACZ (Liebmann *et al.*, 1999; Chaves and Cavalcanti, 2001; Silva and de Carvalho, 2007).

Figure 12 shows the divergence of vertically integrated moisture transport anomalies (DIVQ) during 90th

percentile CEPE events in the WES. While the area of moisture convergence over the NNB during WES is smaller than in the PWS, it is still significantly high. It is interesting to note positive DIVQ anomalies in the tropical Atlantic, suggesting an anomalous southward displacement of the ITCZ from its climatological position.

The pattern of anomalous moisture convergence over the NNB is associated with westerly wind anomalies at 850-hPa over the northern parts of South America

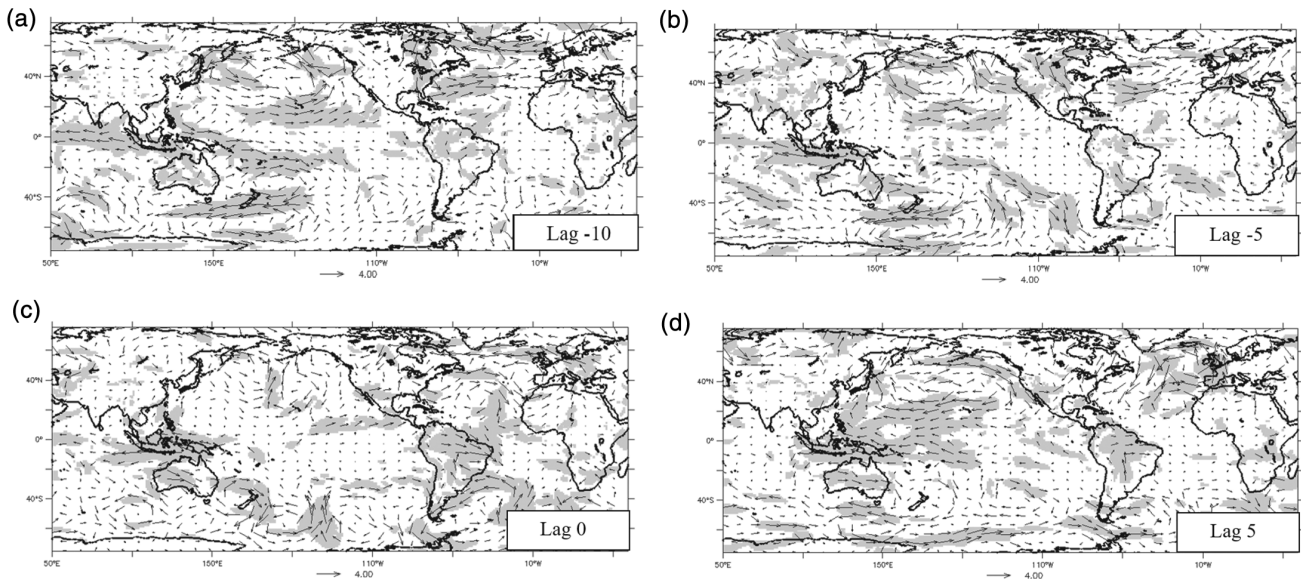


FIGURE 11 Lag composites (days) of wind anomalies at 850 hPa during CEPE in the PWS. (a) Lag -10, (b) lag -5, (c) lag 0, and (d) lag 5. Regions with statistical significance at 5% level are grey colour

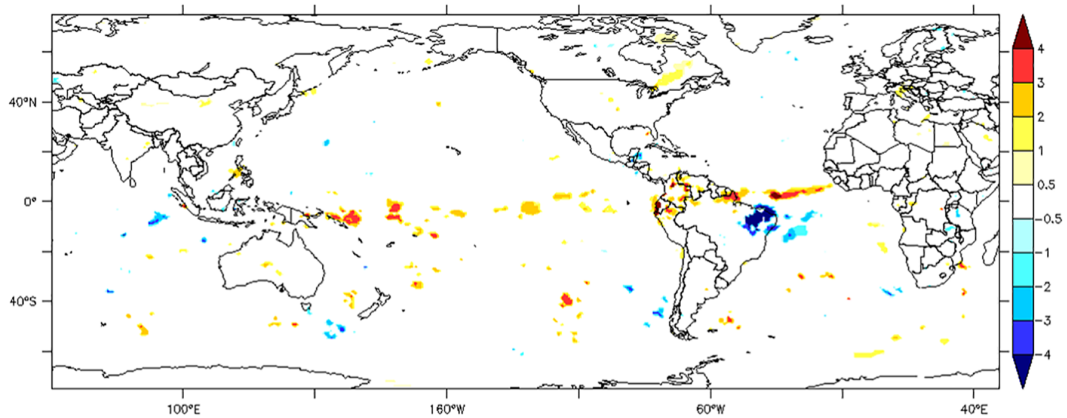
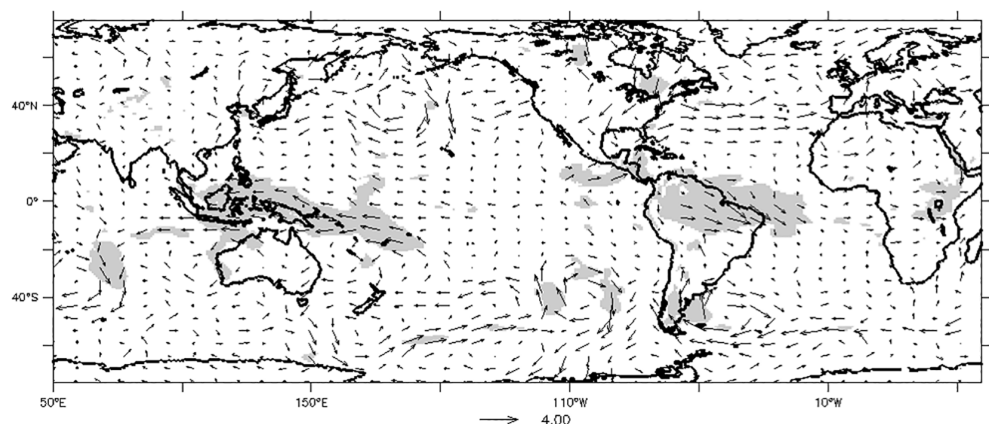


FIGURE 12 Composite of DIVQ anomalies (mm/day) during CEPE for 90th percentile during MJO Phases 8-1-2 during WES. Just points with statistical significance at 5% level are shown [Colour figure can be viewed at wileyonlinelibrary.com]

FIGURE 13 Composites of wind anomalies at 850 hpa during 90th percentile CEPE during MJO Phases 8-2-3 in the WES. Regions with statistical significance at 5% level are grey colour



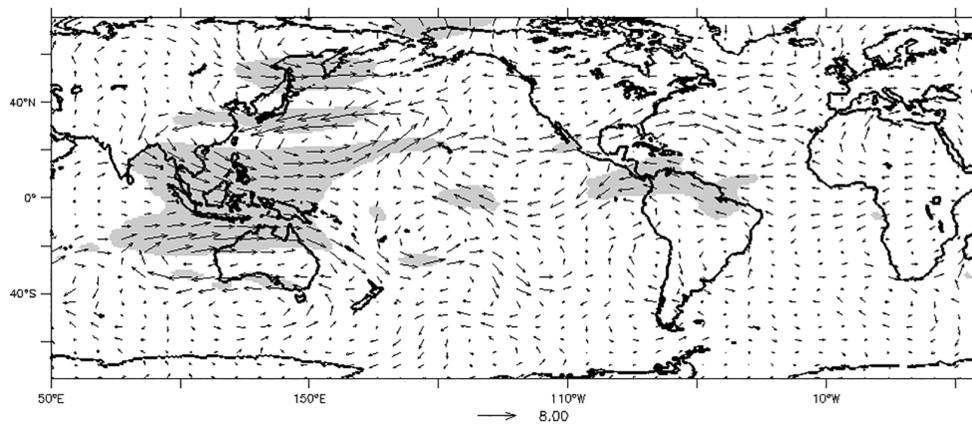


FIGURE 14 As Figure 13 except for wind at 200 hpa

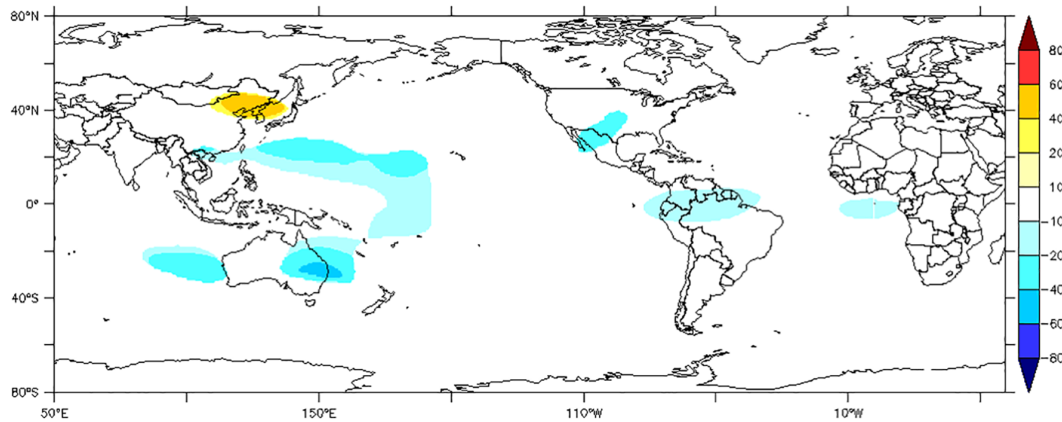


FIGURE 15 As Figure 13 except for H200 (m) [Colour figure can be viewed at wileyonlinelibrary.com]

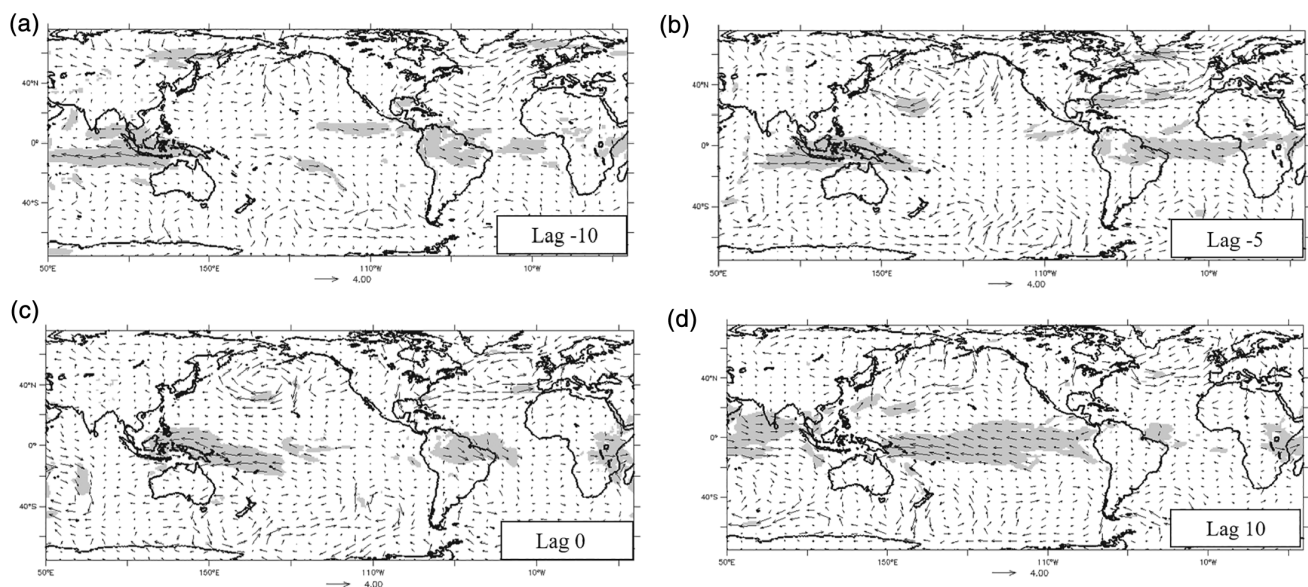


FIGURE 16 Lag composites of wind anomalies ($\text{m}\cdot\text{s}^{-1}$) at 850 hPa during 90th percentile CEPE in the WES. (a) lag -10, (b) lag -5, (c) lag 0, (d) lag 10. Regions with statistical significance at 5% level are in grey colour

(Figure 13). Unlike the results for the PWS, composites of wind anomalies at 200-hPa (Figure 14) and geopotential height anomalies at 200-hPa (Figure 15) do not show wavetrain propagation from the South Pacific Ocean. During WES, the occurrences of 90th percentile CEPE are associated with the equatorial eastward propagation of the MJO.

Figure 16 shows lag composites of wind anomalies at 850-hPa during 90th percentile CEPE in the WES. At lags -10 and -5 days, westerly anomalies progressively shift eastward over the northern parts of South America while easterly anomalies also shift eastward from Indo-Pacific region towards central and eastern Tropical Pacific. At lag 0 days, low-level moisture convergence is maximum over the NNB. At lag $+10$ days, wind anomalies weaken significantly over NNB. MJO changes the lower level circulation as long as it propagates in the equatorial plane, the mechanism associated to very intense and large extreme is related to the weakening of trade winds and vapour transport southward in the vicinity of NNB, which rapidly enhances the water vapour flux convergence and generate the extreme event. The lag composites demonstrate that the MJO influence on extreme precipitation over the NNB in the WES occurs along the equatorial region rather than remotely forced by wavetrain propagation.

4 | CONCLUSIONS

This study investigated the influence of the MJO on extreme precipitation over the NNB. The novel aspect of this study is the characterization of intensity of rainfall and size of contiguous regions of extreme precipitation. In addition, the analysis was performed by separating the PWS and WES precipitation regimes in the NNB. The results show that the MJO significantly controls the occurrences of extreme precipitation over the NNB. This influence is markedly stronger for 90th percentile CEPE events than for 75th CEPE.

In the PWS regime, Rossby waves disturbances propagate over the waveguide from the Indo-Pacific region to central South America and favour the occurrence of extreme precipitation over NNB (and central-southeastern Brazil). Similar patterns were obtained by other studies such as Liebmann *et al.* (1999) and Cunningham and Cavalcanti (2006). In contrast, extreme events in the WES regime are associated with equatorial large-scale circulation anomalies only, mainly related to the eastward propagation of the MJO without subtropical wavetrain propagation. During extreme events during WES, the propagation of convective envelope modifies low-level zonal and meridional circulation over

Equatorial Atlantic near the Brazilian coast, with west anomalies indicating weaker trade winds. That change on trade winds provides moisture flow convergence to incursions southward of the ITCZ over NNB by the enhancement of northern anomalies of water vapour flow.


The influence of the MJO on extreme precipitation over the NNB is distinctively clear in some phases of its life cycle. In the PWS regime, CEPE occurrences are higher in Phases 8, 1, and 2 than in other phases. In the WES regime, CEPE events are more frequent in Phases 8, 2, and 3. In this situation, the eastward propagation of the MJO convective envelope induces low-level westerly wind anomalies that enhance moisture transport convergence and southward displacement of the ITCZ over the NNB.

The MJO is the main mode of tropical intraseasonal variations and its impacts in precipitation variability in the SACZ have been previously documented (e.g., Nogués-Paegle and Mo, 1997; Liebmann *et al.*, 1999; Chaves and Cavalcanti, 2001; Carvalho *et al.*, 2004; Cunningham and Cavalcanti, 2006; Silva and de Carvalho, 2007). Improving MJO monitoring and forecasting is particularly important for northern Northeast Brazil, since extremes precipitation can have significant impacts in poor communities.

ACKNOWLEDGEMENTS

The first author thanks the financial support of FAPESP, process numbers 2011/09314-2 and 2013/09642-5. C. Jones acknowledges the support from NOAA OGP (NA10OAR4310170).

ORCID

Francisco das Chagas Vasconcelos Junior  <https://orcid.org/0000-0002-1558-8383>

REFERENCES

- Aceituno, P. (1988) On the functioning of the southern oscillation in the south American sector. Part I: surface climate. *Monthly Weather Review*, 116(3), 505–524.
- Ambrizzi, T. and Hoskins, B.J. (1997) Stationary Rossby-wave propagation in a baroclinic atmosphere. *Quarterly Journal of the Royal Meteorological Society*, 123(540), 919–928.
- Brito, J.I.B. and Nobre, C.A. (1991) A precipitação da Pré-Estação e a previsibilidade da Estação Chuvosa no Norte do Nordeste. *Climanálise*, 6, 1–8.
- Carvalho, L.M., Jones, C. and Liebmann, B. (2002) Extreme precipitation events in southeastern South America and large-scale convective patterns in the South Atlantic convergence zone. *Journal of Climate*, 15(17), 2377–2394.
- Carvalho, L.M., Jones, C. and Liebmann, B. (2004) The South Atlantic convergence zone: intensity, form, persistence, and relationships with intraseasonal to interannual activity and extreme rainfall. *Journal of Climate*, 17(1), 88–108.
- Cavazos, T. and Rivas, D. (2004) Variability of extreme precipitation events in Tijuana, Mexico. *Climate Research*, 25(3), 229–243.

- Chaves, R.R. and Cavalcanti, I.F.A. (2001) Atmospheric circulation features associated with rainfall variability over southern Northeast Brazil. *Monthly Weather Review*, 129(10), 2614–2626.
- Cunningham, C.C. and Cavalcanti, I.F.A. (2006) Intraseasonal modes of variability affecting the South Atlantic convergence zone. *International Journal of Climatology*, 26, 1165–1180.
- Dee, D.P., Uppala, S.M., Simmons, A.J., Berrisford, P., Poli, P., Kobayashi, S., Andrae, U., Balmaseda, M.A., Balsamo, G., Bauer, P., Bechtold, P., Beljaars, A.C.M., van de Berg, L., Bidlot, J., Bormann, N., Delsol, C., Dragani, R., Fuentes, M., Geer, A.J., Haimberger, L., Healy, S.B., Hersbach, H., Hólm, E. V., Isaksen, I., Kållberg, P., Köhler, M., Matricardi, M., McNally, A.P., Monge-Sanz, B.M., Morcrette, J.-J., Park, B.-K., Peubey, C., de Rosnay, P., Tavolato, C., Thépaut, J.-N. and Vitart, F. (2011) The ERA-interim reanalysis: configuration and performance of the data assimilation system. *Quarterly Journal of the Royal Meteorological Society*, 137(656), 553–597.
- Grimm, A.M. (2019) Madden–Julian oscillation impacts on south American summer monsoon season: precipitation anomalies, extreme events, teleconnections, and role in the MJO cycle. *Climate Dynamics*, 53(1–2), 907–932.
- Grimm, A.M. and Tedeschi, R.G. (2009) ENSO and extreme rainfall events in South America. *Journal of Climate*, 22(7), 1589–1609.
- Hastenrath, S. & Heller, L. (1977) Dynamics of climatic hazards in northeast Brazil. *Q.J.R. Meteorol. Soc.*, 10377–92. <https://doi.org/10.1002/qj.49710343505>.
- Hastenrath, S. (2006) Circulation and teleconnection mechanisms of Northeast Brazil droughts. *Progress in Oceanography*, 70, 407–415.
- Hastenrath, S. (2012) Exploring the climate problems of Brazil's Nordeste: a review. *Climatic Change*, 112(2), 243–251.
- Hastenrath, S. and Lamb, P. (1978) On the dynamics and climatology of surface flow over the equatorial oceans. *Tellus*, 30, 436–448.
- Hendon, H.H. and Liebmann, B. (1990) The Intraseasonal (30–50 day) oscillation of the Australian summer monsoon. *Journal of the Atmospheric Sciences*, 47(24), 2909–2924.
- Jones, C. (2000) Occurrence of extreme precipitation events in California and relationships with the Madden–Julian oscillation. *Journal of Climate*, 13(20), 3576–3587.
- Jones, C. and Carvalho, L.M. (2012) Spatial–intensity variations in extreme precipitation in the contiguous United States and the Madden–Julian oscillation. *Journal of Climate*, 25(14), 4898–4913.
- Jones, C. and Carvalho, L.M. (2014) Sensitivity to Madden–Julian oscillation variations on heavy precipitation over the contiguous United States. *Atmospheric Research*, 147, 10–26.
- Jones, C., Waliser, D.E., Lau, K.M. and Stern, W. (2004) Global occurrences of extreme precipitation and the Madden–Julian oscillation: observations and predictability. *Journal of Climate*, 17(23), 4575–4589.
- Kousky, V.E. (1979) Frontal influences on Northeast Brazil. *Monthly Weather Review*, 107, 1140–1153.
- Kousky, V.E. and Alonso Gan, M. (1981) Upper tropospheric cyclonic vortices in the tropical South Atlantic. *Tellus*, 33(6), 538–551.
- Liebmann, B. and Allured, D. (2005) Daily precipitation grids for South America. *Bulletin of the American Meteorological Society*, 86(11), 1567–1570.
- Liebmann, B., Kiladis, G.N., Allured, D., Vera, C.S., Jones, C., Carvalho, L.M. and Gonzáles, P.L. (2011) Mechanisms associated with large daily rainfall events in Northeast Brazil. *Journal of Climate*, 24(2), 376–396.
- Liebmann, B., Kiladis, G.N., Marengo, J., Ambrizzi, T. and Glick, J. D. (1999) Submonthly convective variability over South America and the South Atlantic convergence zone. *Journal of Climate*, 12(7), 1877–1891.
- Liebmann, B. and Smith, C.A. (1996) Description of a complete (interpolated) outgoing longwave radiation dataset. *Bulletin of the American Meteorological Society*, 77(6), 1275–1277.
- Madden, R.A. and Julian, P.R. (1972) Description of global-scale circulation cells in the tropics with a 40–50 day period. *Journal of the Atmospheric Sciences*, 29(6), 1109–1123.
- Madden, R.A. and Julian, P.R. (1994) Observations of the 40–50-day tropical oscillation—a review. *Monthly Weather Review*, 122(5), 814–837.
- Martin, E.R. and Schumacher, C. (2011) Modulation of Caribbean precipitation by the Madden–Julian oscillation. *Journal of Climate*, 24(3), 813–824.
- Matthews, A.J. (2000) Propagation mechanisms for the Madden–Julian oscillation. *Quarterly Journal of the Royal Meteorological Society*, 126(569), 2637–2651.
- Moura, A.D. and Shukla, J. (1981) On the dynamics of droughts in Northeast Brazil: observations, theory and numerical experiments with a general circulation model. *Journal of the Atmospheric Sciences*, 38(12), 2653–2675.
- Mutai, C.C. and Ward, M.N. (2000) East African rainfall and the tropical circulation/convection on intraseasonal to interannual timescales. *Journal of Climate*, 13, 3915–3939.
- Muza, M.N., Carvalho, L.M., Jones, C. and Liebmann, B. (2009) Intraseasonal and interannual variability of extreme dry and wet events over southeastern South America and the subtropical Atlantic during austral summer. *Journal of Climate*, 22(7), 1682–1699.
- Namias, J. (1972) Influence of northern hemisphere general circulation on drought in Northeast Brazil. *Tellus*, 24, 336–343. <https://doi.org/10.1111/j.2153-3490.1972.tb01561.x>.
- Nogués-Paegle, J. and Mo, K.C. (1997) Alternating wet and dry conditions over South America during summer. *Monthly Weather Review*, 125(2), 279–291.
- Philander, S.G.H. (1983) El Niño southern oscillation phenomena. *Nature*, 302(5906), 295–301.
- Ramos, R.P.L. (1975) Precipitation characteristics in the Northeast Brazil dry region. *Journal of Geophysical Research*, 80(12), 1665–1678.
- Rao, V.B., Giarolla, E., Kayano, M.T. and Franchito, S.H. (2006) Is the recent increasing trend of rainfall over Northeast Brazil related to sub-Saharan drought? *Journal of Climate*, 19(17), 4448–4453.
- Shimizu, M.H. and Ambrizzi, T. (2016) MJO influence on ENSO effects in precipitation and temperature over South America. *Theoretical and Applied Climatology*, 124(1–2), 291–301.
- Silva, A.E. and de Carvalho, L.M.V. (2007) Large-scale index for South America monsoon (LISAM). *Atmospheric Science Letters*, 8(2), 51–57.
- Souza, E.B. & Ambrizzi, T. (2006) Modulation of the intraseasonal rainfall over tropical Brazil by the Madden–Julian oscillation. *International Journal of Climatology: A Journal of the Royal Meteorological Society*, 26(13), 1759–1776.

- Sun, L., Li, H., Zebiak, S.E., Moncunill, D.F., Filho, F.D. and Moura, A.D. (2006) An operational dynamical downscaling prediction system for Nordeste Brazil and the 2002–04 real-time forecast evaluation. *Journal of Climate*, 19(10), 1990–2007.
- Valadão, C.E., Carvalho, L.M., Lucio, P.S. and Chaves, R.R. (2017) Impacts of the Madden-Julian oscillation on intraseasonal precipitation over Northeast Brazil. *International Journal of Climatology*, 37(4), 1859–1884.
- Valadão, C.E., Lucio, P.S., Chaves, R.R. and Carvalho, L.M. (2015) Mjo modulation of station rainfall in the semiarid seridó, Northeast Brazil. *Atmospheric and Climate Sciences*, 5(04), 408–417.
- Vasconcelos Junior, F.C., Jones, C. and Gandu, A.W. (2018) Interannual and intraseasonal variations of the onset and demise of the pre-wet season and the wet season in the northern Northeast Brazil. *Revista Brasileira de Meteorologia*, 33(3), 472–484.
- Wheeler, M.C. and Hendon, H.H. (2004) An all-season real-time multivariate MJO index: development of an index for monitoring and prediction. *Monthly Weather Review*, 132(8), 1917–1932.
- Wilks, D.S. (2011) *Statistical Methods in the Atmospheric Sciences*, Vol. 100 Oxford: Academic press.
- Xavier, P., Rahmat, R., Cheong, W.K. and Wallace, E. (2014) Influence of Madden-Julian oscillation on Southeast Asia rainfall extremes: observations and predictability. *Geophysical Research Letters*, 41, 4406–4412. <https://doi.org/10.1002/2014GL060241>.
- Zhang, C. (2013) Madden–Julian oscillation: bridging weather and climate. *Bulletin of the American Meteorological Society*, 94(12), 1849–1870.
- Zhang, L., Wang, B. and Zeng, Q. (2009) Impact of the Madden-Julian oscillation on summer rainfall in Southeast China. *Journal of Climate*, 22(2), 201–216.

How to cite this article: Vasconcelos Junior FC, Jones C, Gandu AW, Martins ESPR. Impacts of the Madden-Julian Oscillation on the intensity and spatial extent of heavy precipitation events in northern Northeast Brazil. *Int J Climatol*. 2021;41: 3628–3639. <https://doi.org/10.1002/joc.7039>